Journal of Mathematical Modeling
Vol. 9, No. 1, 2021, pp. 1–12

JMM

A moving kriging interpolation-based meshfree method for solving two-phase elasticity system

Ameneh Taleei*

Department of Mathematics, Shiraz University of Technology, Shiraz, Iran

Email(s): a.taleei@sutech.ac.ir

Abstract. The elasticity interface problems occur frequently when two or more materials meet. In this paper, a meshfree point collocation method based on moving kriging interpolation is proposed for solving the two-phase elasticity system with an arbitrary interface. The moving kriging shape function and its derivatives are constructed by moving kriging interpolation technique. Since the shape function possesses the Kronecker delta property then the Dirichlet boundary condition can be implemented directly and easily. Numerical results demonstrate the accuracy and efficiency of the proposed method for the studied problems with constant and variable coefficients.

Keywords: Two-phase elasticity system, meshfree method, moving kriging interpolation (MKI), interface problems.
AMS Subject Classification 2010: 74B05, 65N35, 82B24.

1 Introduction

The elasticity interface problems have attracted a lot of attention from theoretical analysis and numerical studies, see [11, 14–16, 18, 21–23, 34] and the references therein. The elasticity problems of multiple phases of elastic materials separated by phase interfaces arise in many areas, such as the atomic interactions [29], the epitaxial growth of thin films [4], and the crystalline materials [12] problems. The understanding of these physical processes is crucial to improve material stability properties, and in turn to develop new and advanced materials that have many applications in automobile manufacture, aircraft industries, and modern communication technologies [26, 35]. However, solving such elasticity problems is not often easy due to complicated geometries and multiple components that appear in these problems [2, 8, 17].

Meshfree methods have gained much attention in solving the interface problems because they involve simple processing, arbitrary node distribution, and flexibility of placing nodes at

*Corresponding author.
Received: 14 July 2020 / Revised: 24 July 2020 / Accepted: 24 July 2020
DOI: 10.22124/jmm.2020.17088.1484

arbitrary locations [1, 9, 24]. In recent years, a variety of meshfree methods has been studied to the interface problems [5, 10, 19, 20, 27, 28, 33]. As the moving least squares (MLS) scheme is considered a beneficial scheme to approximate discrete data with reasonable accuracy, the meshfree point collocation method based on MLS shape function can be an efficient technique to solve interface problems. However, the approximative nature of the MLS shape functions makes it more difficult to impose the Dirichlet boundary condition due to the lack of Kronecker delta property of the shape functions. An effective way to solve this problem is to use the moving kriging interpolation (MKI) instead of the MLS approximation [13, 32]. The MKI possesses the Kronecker delta function property and the Dirichlet boundary can be implemented directly and easily [6, 25].

Meshfree strong form methods are an attractive alternative to the weak forms. Because these methods do not require any numerical integration to generate the global stiffness matrix. However, the meshfree collocation methods based on MLS numerically suffer from high-order derivatives computations [28]. As is said in [7, 13], the computational cost of derivatives in MKI is lower than MLS approximation. Therefore, the use of MK shape function in the meshfree point collocation method can be computationally effective.

The various of meshless methods based on MKI has been studied to solve elasticity problem [3, 30, 31, 36]. In this paper, the MKI based meshfree point collocation method is studied for solving the two-phase elasticity system. To construct the proper shape function near the interface, an efficient modification of the correlation function in MKI is considered. In this technique, the computational domain disjoints into two subdomains that in each domain, a boundary value problem with a smooth solution is solved. In the proposed method, direct collocation at the nodes is used to impose the Dirichlet boundary condition and the jump conditions.

The structure of the paper is as follows. In the next section, a brief review of the MKI scheme is discussed. Section 3 is devoted to the state of the two-phase elasticity problem. The implement of the MKI based meshfree point collocation method is demonstrated for solving the studied problem in Section 4. Also, in this section, the modification of the correlation function in MKI across the interface is explained. In Section 5, the obtained numerical results are presented. The paper ends by concluding remarks in Section 6.

2 MKI scheme

In this section, a review of the MK interpolation is given. For more details of the MKI, see [13, 32]. Consider a set of n nodes scattered in a domain Ω and $\mathbf{x}_i$ be the coordinates of node i. Let the local approximation $v^h(\mathbf{x})$ of $v(\mathbf{x})$ in a small neighbourhood $\Omega_{\mathbf{x}}$ of $\mathbf{x}$ be as follows

$$v^h(\mathbf{x}) = \boldsymbol{\psi}(\mathbf{x})\mathbf{v}, \qquad \mathbf{x} \in \Omega_{\mathbf{x}}, \tag{1}$$

where $\boldsymbol{\psi}(\mathbf{x}) = [\psi_1(\mathbf{x}), \ldots, \psi_n(\mathbf{x})]$, and $\mathbf{v} = [v_1, v_2, \ldots, v_n]^T$ is a vector of nodal variables. The shape function $\boldsymbol{\psi}(\mathbf{x})$ of MKI is defined as [13]

$$\boldsymbol{\psi}(\mathbf{x}) = \mathbf{p}(\mathbf{x})\mathsf{A} + \mathbf{r}(\mathbf{x})\mathsf{B}, \tag{2}$$

where $\mathbf{p}(\mathbf{x}) = [p_1(\mathbf{x}), p_2(\mathbf{x}), \ldots, p_m(\mathbf{x})]$, $p_j(\mathbf{x})$ $(j = 1, 2, \ldots, m)$ are monomial basis functions, m is the number of terms of the basis. $\mathbf{r}(\mathbf{x})$ is the vector of correlation function between point $\mathbf{x}$

and the given local nodes which are located inside the supporting domain of $\mathbf{x}$,

$$\mathbf{r}(\mathbf{x}) = [\gamma(\mathbf{x}, \mathbf{x}_1), \gamma(\mathbf{x}, \mathbf{x}_2), \ldots, \gamma(\mathbf{x}, \mathbf{x}_n)].$$

The matrices A and B are in the following forms

$$\mathsf{A} = (\mathsf{P}^T\mathsf{R}^{-1}\mathsf{P})^{-1}\mathsf{P}^T\mathsf{R}^{-1},$$

$$\mathsf{B} = \mathsf{R}^{-1}(\mathsf{I} - \mathsf{P}\mathsf{A}),$$

where P and R are the polynomial basis function values matrix and the symmetric correlation matrix, respectively, as follows

$$\mathsf{P} = \begin{bmatrix} p_1(\mathbf{x}_1) & \ldots & p_m(\mathbf{x}_1) \\ p_1(\mathbf{x}_2) & \ldots & p_m(\mathbf{x}_2) \\ \vdots & \ddots & \vdots \\ p_1(\mathbf{x}_n) & \ldots & p_m(\mathbf{x}_n) \end{bmatrix}, \quad \mathsf{R} = \begin{bmatrix} \gamma(\mathbf{x}_1, \mathbf{x}_1) & \ldots & \gamma(\mathbf{x}_1, \mathbf{x}_n) \\ \gamma(\mathbf{x}_2, \mathbf{x}_1) & \ldots & \gamma(\mathbf{x}_2, \mathbf{x}_n) \\ \vdots & \ddots & \vdots \\ \gamma(\mathbf{x}_n, \mathbf{x}_1) & \ldots & \gamma(\mathbf{x}_n, \mathbf{x}_n) \end{bmatrix}.$$

Many functions can be used as a correlation function [13, 37]. In this paper, the quartic spline function is used as the correlation function $\gamma(\mathbf{x}_i, \mathbf{x}_j)$,

$$\gamma(\mathbf{x}_i, \mathbf{x}_j) = \begin{cases} 1 + r_{ij}^2(-6 + 8r_{ij} - 3r_{ij}^2), & r_{ij} \leq 1, \\ 0, & r_{ij} > 1, \end{cases}$$

where $r_{ij} = \frac{||\mathbf{x}_i - \mathbf{x}_j||}{\rho_i}$ and ρ_i is the average distance of the local nodes.

The α^{th} derivative of function $v(\mathbf{x})$ with respect to $\mathbf{x} = (x, y)$ is defined by a differential operator $D^\alpha_{\mathbf{x}} v(\mathbf{x}) := \frac{\partial^\alpha v}{\partial x^{\alpha_1} \partial y^{\alpha_2}}$, where $\alpha = \alpha_1 + \alpha_2$. The derivatives of the approximation (1) are obtained as follows

$$D^\alpha_{\mathbf{x}} v^h(\mathbf{x}) = \big(D^\alpha_{\mathbf{x}}\mathbf{p}(\mathbf{x})\mathsf{A} + D^\alpha_{\mathbf{x}}\mathbf{r}(\mathbf{x})\mathsf{B}\big)\mathbf{v}.$$

It should be noted that the shape function of the MKI possesses the Kronecker delta function property. This property enables meshfree methods to impose the Dirichlet boundary condition directly.

3 The two-phase elasticity problem

Let Ω be an open bounded domain in $\mathbb{R}^2$ which is separated into two subdomains Ω^+ and Ω^- by interface Γ, i.e., $\Gamma = \bar{\Omega}^+ \cap \bar{\Omega}^-$. See Figure 1 for an illustration. It is assumed that the subdomains Ω^+ and Ω^- are occupied by two different elastic materials. In this paper, the two-phase elasticity system is considered in the following form:

$$\nabla.\boldsymbol{\sigma}(\mathbf{u}) + \mathbf{f} = \mathbf{0}, \quad \text{in } \Omega^+ \cup \Omega^-, \tag{3}$$

with the Dirichlet boundary condition

$$\mathbf{u} = \mathbf{g}, \quad \text{on } \partial\Omega, \tag{4}$$

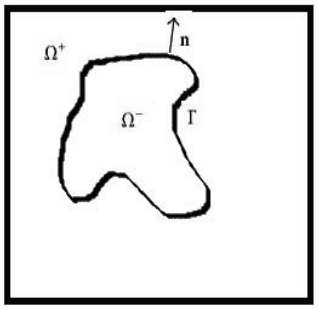

Figure 1: A sketch of the domain for the two-phase elasticity problem with interface Γ.

and the jump conditions

$$[\mathbf{u}]_\Gamma = \mathbf{j_D}, \quad \text{on } \Gamma, \tag{5}$$
$$[\boldsymbol{\sigma}(\mathbf{u}).\mathbf{n}]_\Gamma = \mathbf{j_F}, \quad \text{on } \Gamma. \tag{6}$$

Here, $\boldsymbol{\sigma}$ is the stress tensor. $\mathbf{f} = (f_1, f_2)^T$ is the body force which is known, $\mathbf{u} = (u_1(x,y), u_2(x,y))^T$ is the position of the point (x,y) of the deformed elastic body. The jump $[.]_\Gamma$ is defined as the difference of the limiting values from the outside of the interface to the inside, and $\mathbf{n}$ is the unit normal direction of the interface Γ pointing from the $-$ phase to the $+$ phase. For isotropic elasticity problems, the stress-strain relation is given by $\boldsymbol{\sigma}(\mathbf{u}) = \lambda tr(\boldsymbol{\epsilon}(\mathbf{u}))\mathsf{I} + 2\mu\boldsymbol{\epsilon}(\mathbf{u})$, where $\boldsymbol{\epsilon}(\mathbf{u}) = \frac{1}{2}\big(\nabla\mathbf{u} + (\nabla\mathbf{u})^T\big)$ is the strain tensor with the trace being $tr(\boldsymbol{\epsilon}(\mathbf{u})) = \sum_{i,j}\epsilon_{i,j}(\mathbf{u})$. The Lame parameters λ and μ can be constant or spatial dependent functions. The physical parameters have a finite jump discontinuity as follows

$$(\lambda, \mu) = \begin{cases} (\lambda^+, \mu^+), & \text{in } \Omega^+, \\ (\lambda^-, \mu^-), & \text{in } \Omega^-. \end{cases}$$

The equations (3)-(6) can be written in the component-wise form as follows,

$$\begin{aligned} (\lambda+2\mu)\frac{\partial^2 u_1}{\partial x^2} + \mu\frac{\partial^2 u_1}{\partial y^2} + (\lambda_x + 2\mu_x)\frac{\partial u_1}{\partial x} + \mu_y\frac{\partial u_1}{\partial y} & \\ +(\lambda+\mu)\frac{\partial^2 u_2}{\partial x\partial y} - \mu_y\frac{\partial u_2}{\partial x} - \lambda_x\frac{\partial u_2}{\partial y} &= -f_1, \quad \text{in } \Omega^\pm, \end{aligned} \tag{7}$$

$$\begin{aligned} (\lambda+\mu)\frac{\partial^2 u_1}{\partial x\partial y} + \lambda_y\frac{\partial u_1}{\partial x} + \mu_x\frac{\partial u_1}{\partial y} + \mu\frac{\partial^2 u_2}{\partial x^2} & \\ +(\lambda+2\mu)\frac{\partial^2 u_2}{\partial y^2} + \mu_x\frac{\partial u_2}{\partial x} + (\lambda_y + 2\mu_y)\frac{\partial u_2}{\partial y} &= -f_2, \quad \text{in } \Omega^\pm, \end{aligned} \tag{8}$$

$$(u_1, u_2) = (g_1, g_2), \quad \text{on } \partial\Omega, \tag{9}$$
$$[(u_1, u_2)] = (j_{D1}, j_{D2}), \quad \text{on } \Gamma, \tag{10}$$
$$\left[(\lambda+2\mu)\, n_1\frac{\partial u_1}{\partial x} + \mu n_2\frac{\partial u_1}{\partial y} + \mu n_2\frac{\partial u_2}{\partial x} + \lambda n_1\frac{\partial u_2}{\partial y}\right] = j_{F1}, \quad \text{on } \Gamma, \tag{11}$$
$$\left[\lambda n_2\frac{\partial u_1}{\partial x} + \mu n_1\frac{\partial u_1}{partialy} + \mu n_1\frac{\partial u_2}{\partial x} + (\lambda+2\mu)n_2\frac{\partial u_2}{\partial y}\right] = j_{F2}, \quad \text{on } \Gamma. \tag{12}$$

4 Numerical method

In the proposed method, the governing equations, the boundary condition, and the jump conditions are discretized by the collocation technique. Before the discretization of the governing equations, first, the modification of the MK shape function is explained across the interface Γ.

Consider the domain Ω consisting of two different materials separated by the interface Γ. To modify the MKI's correlation function, the collocation nodes are split into two sets Λ^+ and Λ^-, where $\Lambda^+(\Lambda^-)$ shows the set of nodes that belong exclusively to the subdomain $\bar{\Omega}^+(\bar{\Omega}^-)$. To create the proper discontinuity in the shape function across the interface, the modification of correlation function in MKI is considered as follows

$$\gamma^{\pm}(\mathbf{x}_i,\mathbf{x}_j)=\begin{cases}\gamma(\mathbf{x}_i,\mathbf{x}_j), & \mathbf{x}_i,\mathbf{x}_j\in\Lambda^{\pm},\\ 0, & \text{otherwise.}\end{cases} \tag{13}$$

It is easy to see that in this technique, nodes from a subdomain are not required to influence the other. As the support domain of a point in a subdomain contains only nodes from the same subdomain. However, the support domain of a point on Γ contains nodes from Λ^+ and Λ^-. Thus two sets of nodes are assigned on the interface Γ at the same location, but with different material properties.

Substituting Eq. (13) into Eq. (1), the approximation value of v^h can be expressed in the following form

$$v^h(\mathbf{x})=v^{h\pm}(\mathbf{x})=\sum_{i=1}^{N_{\Lambda^{\pm}}}\psi_i^{\pm}(\mathbf{x})v_i^{\pm},\quad \mathbf{x}\in\bar{\Omega}^{\pm},$$

where $N_{\Lambda^{\pm}}$ is the number of nodes in $\bar{\Omega}^{\pm}$.

Let $\mathbf{u}^{h\pm}=(u_1^{h\pm},u_2^{h\pm})^T$ in Eqs. (7)-(12). The strategy in the collocation method is simultaneously solving equations (7)-(12). Collocating (7)-(8) at the interior points $\Lambda_I^{\pm}$, (9) at the boundary points Λ_b and (10)-(12) at the interface points Λ_Γ, leads to the following system

$$\begin{aligned}
&\sum_{i=1}^{N_{\Lambda^{\pm}}}\Big(\big((\lambda^{\pm}+2\mu^{\pm})(\mathbf{x}_j)\psi_{i,xx}^{\pm}(\mathbf{x}_j)+\mu^{\pm}(\mathbf{x}_j)\psi_{i,yy}^{\pm}(\mathbf{x}_j)+(\lambda_x^{\pm}+2\mu_x^{\pm})(\mathbf{x}_j)\psi_{i,x}^{\pm}(\mathbf{x}_j)\\
&\qquad+\mu_y^{\pm}(\mathbf{x}_j)\psi_{i,y}^{\pm}(\mathbf{x}_j)\big)u_{1,i}^{\pm}+\big((\lambda^{\pm}+\mu^{\pm})(\mathbf{x}_j)\psi_{i.xy}^{\pm}(\mathbf{x}_j)-\mu_y^{\pm}(\mathbf{x}_j)\psi_{i,x}^{\pm}(\mathbf{x}_j)\\
&\qquad-\lambda_x^{\pm}(\mathbf{x}_j)\psi_{i,y}^{\pm}(\mathbf{x}_j)\big)u_{2,i}^{\pm}\Big)=-f_1^{\pm}(\mathbf{x}_j),\quad \mathbf{x}_j\in\Lambda_I^{\pm},
\end{aligned}\tag{14}$$

$$\begin{aligned}
&\sum_{i=1}^{N_{\Lambda^{\pm}}}\Big(\big((\lambda^{\pm}+\mu^{\pm})(\mathbf{x}_j)\psi_{i,xy}^{\pm}(\mathbf{x}_j)+\lambda_y^{\pm}(\mathbf{x}_j)\psi_{i,x}^{\pm}(\mathbf{x}_j)+\mu_x^{\pm}(\mathbf{x}_j)\psi_{i,y}^{\pm}(\mathbf{x}_j)\big)u_{1,i}^{\pm}\\
&\qquad+\big(\mu^{\pm}(\mathbf{x}_j)\psi_{i,xx}^{\pm}(\mathbf{x}_j)+(\lambda^{\pm}+2\mu^{\pm})(\mathbf{x}_j)\psi_{i.yy}^{\pm}(\mathbf{x}_j)+\mu_x^{\pm}(\mathbf{x}_j)\psi_{i,x}^{\pm}(\mathbf{x}_j)\\
&\qquad+(\lambda_y^{\pm}+2\mu_y^{\pm})(\mathbf{x}_j)\psi_{i,y}^{\pm}(\mathbf{x}_j)\big)u_{2,i}^{\pm}\Big)=-f_2^{\pm}(\mathbf{x}_j),\quad \mathbf{x}_j\in\Lambda_I^{\pm},
\end{aligned}\tag{15}$$

$$(u_{1,j}^{+},u_{2,j}^{+})=(g_1(\mathbf{x}_j),g_2(\mathbf{x}_j)),\quad \mathbf{x}_j\in\Lambda_b,\tag{16}$$

$$(u_{1,j}^{+},u_{2,j}^{+})-(u_{1,j}^{-},u_{2,j}^{-})=(j_{D1}(\mathbf{x}_j),j_{D2}(\mathbf{x}_j)),\quad \mathbf{x}_j\in\Lambda_\Gamma,\tag{17}$$

$$\sum_{i=1}^{N_{\Lambda^+}}\Big(\big((\lambda^+ + 2\mu^+)(\mathbf{x}_j)n_1^+\psi_{i,x}^+(\mathbf{x}_j) + \mu^+(\mathbf{x}_j)n_2^+\psi_{i,y}^+(\mathbf{x}_j)\big)u_{1,i}^+ + \big(\mu^+(\mathbf{x}_j)n_2^+ \psi_{i,x}^+(\mathbf{x}_j) + \lambda^+(\mathbf{x}_j)n_1^+\psi_{i,y}^+(\mathbf{x}_j)\big)u_{2,i}^+\Big) - \sum_{i=1}^{N_{\Lambda^-}}\Big(\big((\lambda^- + 2\mu^-)(\mathbf{x}_j)n_1^- \psi_{i,x}^-(\mathbf{x}_j) + \mu^-(\mathbf{x}_j)n_2^-\psi_{i,y}^-(\mathbf{x}_j)\big)u_{1,i}^- + \big(\mu^-(\mathbf{x}_j)n_2^-\psi_{i,x}^-(\mathbf{x}_j) - \lambda^-(\mathbf{x}_j) n_1^-\psi_{i,y}^-(\mathbf{x}_j)\big)u_{2,i}^-\Big) = j_{F1}(\mathbf{x}_j), \quad \mathbf{x}_j \in \Lambda_\Gamma, \tag{18}$$

$$\sum_{i=1}^{N_{\Lambda^+}}\Big(\big(\lambda^+(\mathbf{x}_j)n_2^+\psi_{i,x}^+ + \mu^+(\mathbf{x}_j)n_1^+\psi_{i,y}^+\big)u_{1,i}^+ + \big(\mu^+(\mathbf{x}_j)n_1^+\psi_{i,x}^+ + (\lambda^+ + 2\mu^+)(\mathbf{x}_j) n_2^+\psi_{i,y}^+\big)u_{2,i}^+\Big) - \sum_{i=1}^{N_{\Lambda^-}}\Big(\big(\lambda^-(\mathbf{x}_j)n_2^-\psi_{i,x}^- + \mu^-(\mathbf{x}_j)n_1^-\psi_{i,y}^-\big)u_{1,i}^- + \big(\mu^-(\mathbf{x}_j)n_1^- \psi_{i,x}^- + (\lambda^- + 2\mu^-)(\mathbf{x}_j)n_2^-\psi_{i,y}^-\big)u_{2,i}^-\Big) = j_{F2}(\mathbf{x}_j), \quad \mathbf{x}_j \in \Lambda_\Gamma, \tag{19}$$

The system (14) -(19) can be written in the following matrix-vector form

$$\mathbf{KU} = \mathbf{F}, \tag{20}$$

where $\mathbf{K}$ is the coefficients matrix of size $2(N_{\Lambda^+} + N_{\Lambda^-}) \times 2(N_{\Lambda^+} + N_{\Lambda^-})$ and also the vectors of $\mathbf{U} = [\mathbf{U}_1, \mathbf{U}_2]^T$, $\mathbf{F} = [\mathbf{F}_1, \mathbf{F}_2]^T$ are as follows

$$\mathbf{U}_l = [u_l^-(\mathbf{X}_\Gamma), u_l^-(\mathbf{X}_{\Lambda_I^-}), u_l^+(\mathbf{X}_\Gamma), u_l^+(\mathbf{X}_{\Lambda_I^+}), u_l^+(\mathbf{X}_{\Lambda_b})],$$
$$\mathbf{F}_l = [j_{Dl}(\mathbf{X}_\Gamma), f_l^-(\mathbf{X}_{\Lambda_I^-}), j_{Fl}(\mathbf{X}_\Gamma), f_l^+(\mathbf{X}_{\Lambda_I^+}), g_l(\mathbf{X}_{\Lambda_b})], \quad l = 1, 2.$$

Note that the vector of $w(\mathbf{Y}_p)$ is defined as $w(\mathbf{Y}_p) = [w(y_1), w(y_2), \ldots, w(y_{N_P})]$, in which $\mathbf{Y}_p = [y_1, y_2, \ldots, y_{N_P}]$. By solving (20), the values of displacement function $\mathbf{u}^h$ are found at the inner points and points on the interface Γ.

5 Numerical experiments

In the current work, three numerical examples are presented to demonstrate the efficiency and accuracy of the proposed method. In all of them, the computational domain Ω is the rectangular region $[-1, 1] \times [-1, 1]$ with interface Γ within the domain. To discretize the computational domain, firstly, a set of regularly or irregularly distributed nodes in Ω is distributed. Then the nodes located on or very closed to the interface are removed. Finally, a set of regularly distributed nodes is placed on the interface Γ and the boundary $\partial\Omega$. Note that in regular distribution, n_x and n_y are the number of grid points in the $x-$ and $y-$ directions, respectively. The shifted and scaled quadratic polynomial basis functions are used to stabilize the MKI scheme [32] where a quadratic polynomial basis function is considered.

Example 1. In this example, a two-phase elasticity problem is studied with the piecewise constant physical parameters and the ellipse interface. The interface is the zero set of $L(x, y) =$

$x^2/4+y^2-r_0$. The Dirichlet boundary condition and the interface conditions are obtained from the following exact solution

$$(u_1(x,y),u_2(x,y)) = (1/\mu L(x,y)x, 1/\mu L(x,y)y).$$

This example is studied with two sets of physical parameters λ, μ, and radii of the interface r_0. Tables 1 and 2 show the convergence behavior of the proposed method with $(\lambda^+,\lambda^-,\mu^+,\mu^-,r_0) =$

Table 1: The values of error in Example 1 for $(\lambda^+,\lambda^-,\mu^+,\mu^-,r_0) = (20,2,10,1,0.4)$.

$n_x \times n_y$	10×10	20×20	40×40	80×80
$L_\infty(\mathbf{u})$	9.71e-3	3.65e-3	9.97e-4	3.05e-4
$L_2(\mathbf{u})$	1.25e-2	2.72e-3	8.15e-4	2.27e-4

Table 2: The values of error in Example 1 for $(\lambda^+,\lambda^-,\mu^+,\mu^-,r_0) = (500,5,100,1,0.3)$.

$n_x \times n_y$	16×16	32×32	64×64	128×128
$L_2(\mathbf{u})$	2.52e-3	6.15e-4	1.03e-4	3.91e-5
$L_2(\mathbf{u})$ [18]	2.02e-3	6.64e-4	1.38e-4	2.74e-5

$(20,2,10,1,0.4)$, $(\lambda^+,\lambda^-,\mu^+,\mu^-,r_0) = (500,5,100,1,0.3)$, respectively. In Table 2, the obtained errors are also compared with those obtained by [18]. Figure 2 plots the numerical displacement solutions of u_1 and u_2 with $(\lambda^+,\lambda^-,\mu^+,\mu^-,r_0) = (20,2,10,1,0.4)$ and $n_x = n_y = 80$.

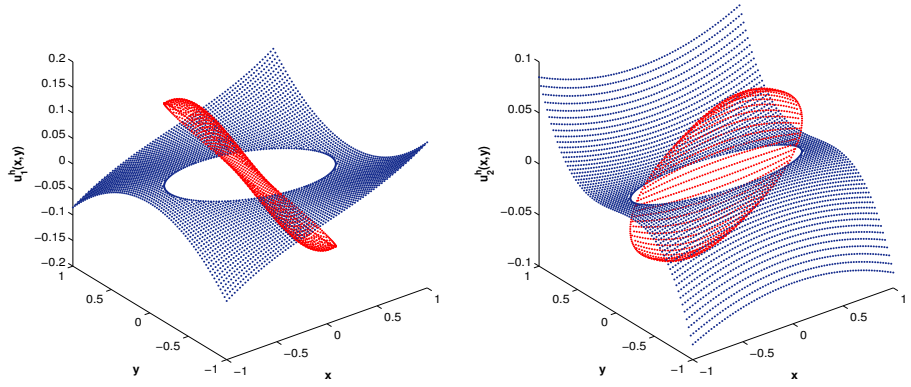

Figure 2: The plots of computed displacement solutions $u_1^h(x,y)$ and $u_2^h(x,y)$ in Example 1.

Example 2. In this example, the behavior of the proposed method is investigated for the two-phase elasticity problem with variable physical parameters and the interface $x^2+y^2 = 0.25$. The physical parameters λ and μ are considered as follows

$$\begin{pmatrix}\lambda^+\\ \lambda^-\end{pmatrix} = \begin{pmatrix}5000000+2000000(x+y)\\ 3000000+2500000xy\end{pmatrix}, \begin{pmatrix}\mu^+\\ \mu^-\end{pmatrix} = \begin{pmatrix}2500000+3000000(x+y)\\ 3000000+2500000xy\end{pmatrix},$$

The Dirichlet boundary condition and the interface conditions are obtained from the following exact solution

$$\begin{pmatrix} u_1^+ \\ u_1^- \end{pmatrix} = \begin{pmatrix} -(r^4 + c_0 \log(2r))/10 - r_0^2 + (r_0^4 + c_0 \log(2r_0))/10 \\ -r^2 \end{pmatrix},$$

$$\begin{pmatrix} u_2^+ \\ u_2^- \end{pmatrix} = \begin{pmatrix} \log(1 + x^2 + 3y^2) + \sin(xy) - 4r^2 + 4r_0^2 \\ \log(1 + x^2 + 3y^2) + \sin(xy) \end{pmatrix},$$

where $r_0 = 0.5,\ c_0 = -0.1$.

Table 3: The values of error in Example 2.

$n_x \times n_y$	10×10	20×20	40×40	80×80
$L_\infty(\mathbf{u})$	5.75e-2	9.25e-3	3.47e-3	6.52e-4
$L_\infty(\mathbf{u})$ [34]	-	1.01e-2	5.54e-3	3.47e-4

Table 3 presents the convergence behavior of the proposed method and also the numerical results have been compared with the reported numerical results in [34]. Figure 3 plots the numerical displacement solutions of u_1 and u_2 with $n_x = n_y = 80$.

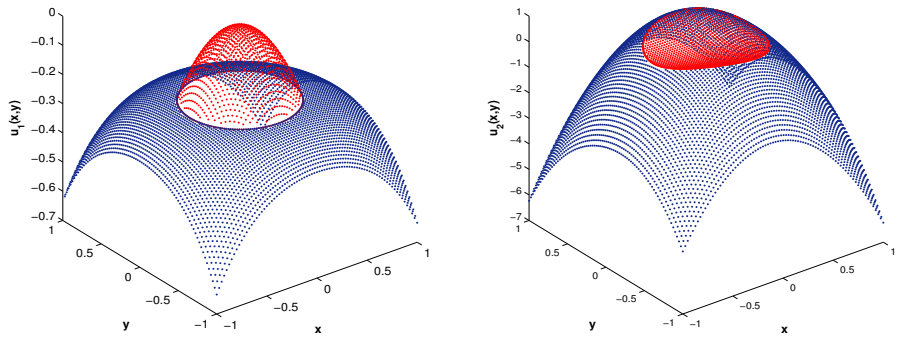

Figure 3: The plots of computed displacement solutions $u_1^h(x, y)$ and $u_2^h(x, y)$ in Example 2.

Example 3. As testing of the proposed method for the two-phase elasticity problem with a more complex interface, flower shape is considered in the polar coordinate $r = 0.5 + \frac{\sin 5\theta}{7}$. The Dirichlet boundary condition and the interface conditions are obtained from the following exact solution

$$\begin{pmatrix} u_1^+ \\ u_1^- \end{pmatrix} = \begin{pmatrix} \exp(-3.5^2(x^2 + y^2)^5) \\ \exp(-(7(x^2 + y^2)^3 - 5x^4y + 10x^2y^3 - y^5)^2) \end{pmatrix},$$

$$\begin{pmatrix} u_2^+ \\ u_2^- \end{pmatrix} = \begin{pmatrix} \exp(-3.5^2(x^2 + y^2)^5) + xy \\ \exp(-(7(x^2 + y^2)^3 - 5x^4y + 10x^2y^3 - y^5)^2) + xy \end{pmatrix},$$

In this example, the two-phase elasticity problem is solved with regularly and irregularly distributed nodes with $(\lambda^+, \lambda^-, \mu^+, \mu^-) = (5, 1, 10, 2)$. The achieved errors of both node distributions are reported in Table 4. Figures 4 and 5 show the plots of the computed solution with $(N_{\Lambda^+}, N_{\Lambda^-}) = (5425, 1482)$ with regularly and irregularly distributed nodes, respectively.

Table 4: The values of error in Example 3.

$(N_{\Lambda^+}, N_{\Lambda^-})$	(143, 61)	(427, 135)	(1395, 358)	(5425, 1482)
$L_\infty(\mathbf{u})$\{regular distribution\}	3.20e-2	6.32e-3	2.49e-3	9.22e-4
$L_\infty(\mathbf{u})$\{irregular distribution\}	2.09e-2	5.71e-3	1.80e-3	6.71e-4

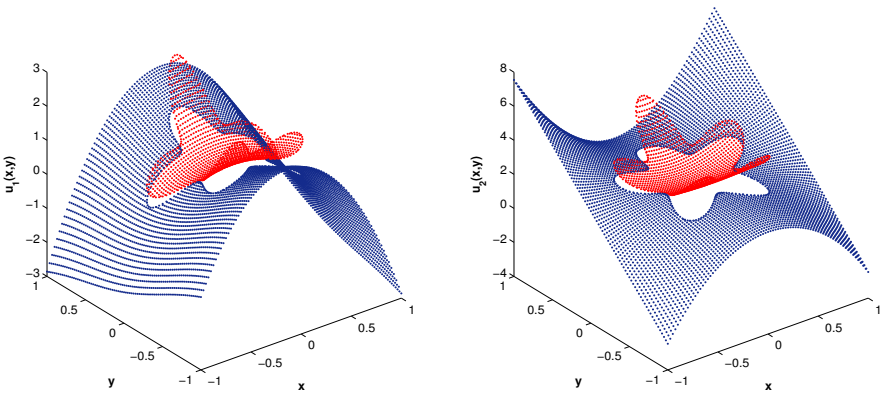

Figure 4: The plots of computed displacement solutions $u_1^h(x, y)$ and $u_2^h(x, y)$ in Example 3 (regular distribution).

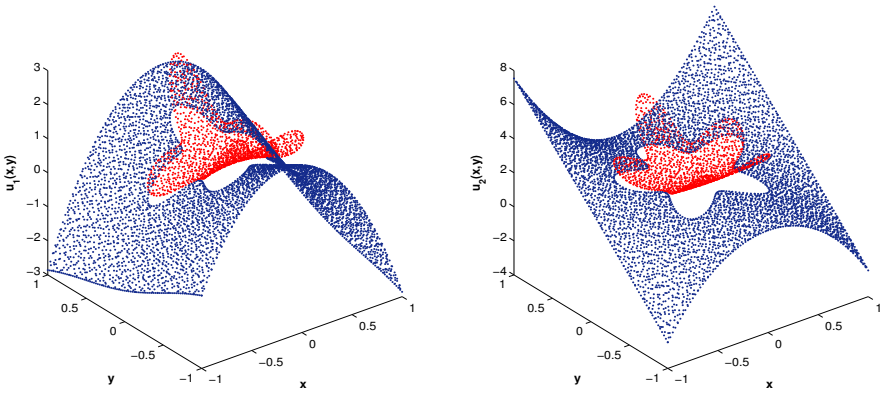

Figure 5: The plots of computed displacement solutions $u_1^h(x, y)$ and $u_2^h(x, y)$ in Example 3 (irregular distribution).

6 Conclusion

In this paper, a simple and effective meshfree point collocation method was proposed to simulate the elasticity interface problems. The developed MKI shape function was considered as the basis function in the proposed method. The correlation function correction was used to construct the appropriate shape functions across the interface. As the MKI has the Kronecker delta property then the Dirichlet boundary condition was imposed directly and easily. The performance of the proposed method was investigated for some test problems with constant and variable physical parameters. The obtained numerical results were also compared with some numerical techniques in the literature. The numerical results also confirmed that the proposed method for the simulation of elasticity problems with a complex interface can be accurate and effective.

References

[1] M. Abbaszadeh, M. Dehghan, *Direct meshless local Petrov-Galerkin method to investigate anisotropic potential and plane elastostatic equations of anisotropic functionally graded materials problems*, Eng. Anal. Bound. Elem. **118** (2020) 188-201.

[2] R.J. Atkin, N. Fox, *An introduction to the theory of elaticity*, Longman, London, 1980.

[3] Y.H. Chen, M.H. Aliabadi, *Meshfree-based micromechanical modelling of twill woven composites*, Compos. Part B-Eng. 197 (2020) 108190.

[4] C-H Chiu, *The model of eye-shaped voids: Elasticity solution and its applications in material failures via morphological transformation*, J. Mech. Phys. Solids. **137** (2020) 103822.

[5] M. Dehghan, M. Abbaszadeh, *Interpolating stabilized moving least squares (MLS) approximation for 2D elliptic interface problems*, Comput. Methods Appl. Mech. Engrg. **328** (2018) 775-803.

[6] M. Dehghan, M. Abbaszadeh, *The solution of nonlinear Green-Naghdi equation arising in water sciences via a meshless method which combines moving kriging interpolation shape functions with the weighted essentially nonoscillatory method*, Commun. Nonlinear Sci. Numer. Simul. **68** (2019) 220-239.

[7] M. Dehghan, N. Narimani, *The element-free Galerkin method based on moving least squares and moving Kriging approximations for solving two-dimensional tumor-induced angiogenesis model*, Engrg. Comput. (2019), https://doi.org/10.1007/s00366-019-00779-0.

[8] T. Fan, *Mathmatical theory of elasticity of quasicrystals and its applications*, Berlin, Heidelberg: Springer-Verlag, Berlin Heidelberg, 2011.

[9] S. Garg, M. Pant, *Meshfree methods: a comprehensive review of applications*, Int. J. Comput. Methods. **15** (2018) 1830001.

[10] F. Gholampour, E. Hesameddini, A.Taleei, *A global RBF-QR collocation technique for solving two-dimensional elliptic problems involving arbitrary interface*, Engrg. Comput. (2020). https://doi.org/10.1007/s00366-020-01013-y

[11] Y. Gong, Z. Li, *Immersed interface finite element methods for elasticity interface problems with non-homogeneous jump conditions*, Numer. Math. Theor. Meth. Appl. **3** (2010) 23-39.

[12] M.A. Grekov, T.S. Sergeeva, *Interaction of edge dislocation array with bimaterial interface incorporating interface elasticity*, Internat. J. Engrg. Sci. **149** (2020) 103233.

[13] L. Gu, *Moving kriging interpolation and element-free Galerkin method*, Internat. J. Numer. Methods Engrg. **56** (2003) 1-11.

[14] R. Guo, T. Lin, Y. Lin, *Error estimates for a partially penalized immersed finite element method for elasticity interface problems*, Math. Model. Numer. Anal. **4** (2020) 1-24.

[15] S. Hou, Z. Li, L. Wang, W. Wang, *A numerical method for solving elasticity equations with interfaces*, Commun. Comput. Phys. **12** (2012) 595-612.

[16] P. Huang, Z. Li, *Partially penalized IFE methods and convergence analysis for elasticity interface problems*, J. Comput. Appl. Math. **382** (2021) 113059.

[17] A. Javili, N.S. Ottosen, J. Mosler, *Aspects of interface elasticity theory*, Math. Mech. Solids. (2017) 1-21.

[18] G. Jo, D.Y. Kwak, *Recent development of immersed FEM for elliptic and elastic interface problems*, J. Korean Soc. Ind. Appl. Math. **23** (2019) 65-92.

[19] S.U. Islam, M. Ahmad, *Meshless analysis of elliptic interface boundary value problems*, Eng. Anal. Bound. Elem. **92** (2018) 38-49.

[20] Z. Jannesari, M. Tatari, *Element free Galerkin method to the interface problems with application in electrostatic*, Int. J. Numer. Model. **29** (2016) 1089-1105.

[21] S. Jin, D.Y. Kwak, D. Kyeong, *A consistent immersed finite element method for the interface elasticity problems*, Adv. Math. Phys. (2016) Article ID 3292487.

[22] D.Y. Kwak, S. Ji, D. Kyeong, *A stabilized P1-nonconforming immersed finite element method for the interface elasticity problems*, ESAIM-Math. Model. Num. **51** (2017) 187-207.

[23] T. Lin, D. Sheen, X. Zhang, *A locking-free immersed finite element method for planar elasticity interface problems*, J. Comput. Phys. **247** (2013) 228-247.

[24] G. R. Liu, *An overview on meshfree methods: for computational solid mechanics*, Int. J. Comput. Methods. **13** (2016) 1630001.

[25] V. Mohammadi, M. Dehghan, A.R. Khodadadian, T. Wick, *Numerical investigation on the transport equation in spherical coordinates via generalized moving least squares and moving kriging least squares approximations*, Engrg. Comput. (2019), https://doi.org/10.1007/s00366-019-00881-3

[26] P. Samadian, C. Butcher, M. J. Worswick, *New mean-field homogenization schemes for the constitutive modelling of the elastic and elastoplastic deformation behavior of multi-phase materials*, Mater. Today Commun. **24** (2020) 100707.

[27] A. Taleei, M. Dehghan, *Direct meshless local Petrov-Galerkin method for elliptic interface problems with applications in electrostatic and elastostatic*, Comput. Methods Appl. Mech. Engrg. **278** (2014) 479-498.

[28] A. Taleei, M. Dehghan, *An efficient meshfree point collocation moving least squares method to solve the interface problems with nonhomogeneous jump conditions*, Numer. Methods Partial Differential Equations, **31** (2015) 1031-1053.

[29] S.M. Teus, V.G. Gavriljuk, *On a correlation between hydrogen effects on atomic interactions and mobility of grain boundaries in the alpha-iron. Stage II. Mobility of grain boundaries in the H-charged α-iron*, Mater. Lett. **259** (2020) 126859.

[30] C.H. Thai, T.N. Nguyen, T. Rabczuk, H. Nguyen-Xuan, *An improved moving Kriging meshfree method for plate analysis using a refined plate theory*, Compos. Struct. **176** (2016) 34-49.

[31] P. Tongsuk, W. Kanok-Nukulchai, *Further investigation of element free Galerkin method using moving kriging interpolation*, Int. J. Comput. Methods. **1** (2004) 345-365.

[32] S. Tu, H. Yang, L.L. Dong, Y. Huang, *A stabilized moving Kriging interpolation method and its application in boundary node boundary*, Eng. Anal. Bound. Elem. **100** (2019) 14-23.

[33] Z. Wang, Z. Zhang, *A mesh-free method for interface problems using the deep learning approach*, J. Comput. Phys. **400** (2020) 108963.

[34] B. Wang, K. Xia, G-W Wei, *Matched interface and boundary method for elasticity interface problems*, J. Comput. Appl. Math. **285** (2015) 203-225.

[35] J. Wilmers, A. McBride, S. Bargmann, *Interface elasticity effects in polymer-filled nanoporous metals*, J. Mech. Phys. Solids.**99** (2017) 163-177.

[36] L.W. Zhang, P. Zhu, K.M. Liew, *Thermal buckling of functionally graded plates using a local Kriging meshless method*, Compos. Struct. **108** (2014) 472-492.

[37] B. Zheng, B. Dai, *A meshless local moving Kriging method for two-dimensional solids*, Appl. Math. Comput. **218** (2011) 563-573.